

1 **Ocean acidification alters phytoplankton diversity and community structure in the coastal**
2 **water of the East China Sea**

3 Yuming Rao^{#1}, Na Wang^{#2}, He Li³, Jiazhen Sun², Xiaowen Jiang², Di Zhang², Liming Qu², Qianqian
4 Fu², Xuyang Wang², Cong Zhou², Zichao Deng², Yang Tian², Xiangqi Yi², Ruiping Huang², Guang
5 Gao², Xin Lin² and Kunshan Gao^{*1,3}

6 ¹ State Key Laboratory of Marine Environmental Science, College of the Environment and Ecology,
7 Xiamen University, Xiamen, China

8 ² State Key Laboratory of Marine Environmental Science, College of Ocean and Earth Science,
9 Xiamen University, Xiamen, China

10 ³ Co-Innovation Center of Jiangsu Marine Bio-industry Technology, Jiangsu Ocean University,
11 Lianyungang 222005, China

12 [#] These authors contributed equally to this work

13 ^{*} Correspondence: ksgao@xmu.edu.cn

14 **Keywords:** CO₂, East China Sea, mesocosms; ocean acidification; phytoplankton; primary
15 production

16 **Abstract**

17 Anthropogenic CO₂ emissions and their continuous dissolution into seawater lead to seawater
18 pCO₂ rise and ocean acidification (OA). Phytoplankton groups are known to be differentially
19 affected by carbonate chemistry changes associated with OA in different regions of contrasting
20 physical and chemical features. To explore responses of phytoplankton to OA in the Chinese coastal
21 waters, we conducted a mesocosm experiment in a eutrophic bay of the southern East China Sea
22 under ambient (410 μatm, AC) and elevated (1000 μatm, HC) pCO₂ levels. The HC condition
23 stimulated phytoplankton growth and primary production during the initial nutrient-replete stage,
24 while the community diversity and evenness in both pCO₂ treatments were reduced during this stage
25 due to the rapid nutrient consumption and diatom blooms, and the subsequent shift from diatoms to
26 hetero-dinoflagellates led to a decline in primary production during the mid and later phases under
27 nutrient depletion. HC treatment suppressed the diatom-to-dinoflagellate succession and enhanced
28 the subsequent remineralization of organic matter, thereby facilitating smaller phytoplankton to
29 dominant and sustaining primary production. Our findings indicate that, the impacts of OA on

删除了: conditions

删除了: Such suppression of

删除了: occurred with enhanced

删除了: under the HC conditions,

删除了: with

删除了: becoming

删除了: for the

删除了: ed

38 phytoplankton diversity in the coastal water of the southern East China Sea depend on availability
39 of nutrients, with primary productivity and biodiversity of phytoplankton reduced in the
40 eutrophicated coastal water.

41 **1 Introduction**

42 It is commonly known that sequestration of CO₂ in coastal waters play important roles against
43 global warming due to their high primary productivity (Rogelj et al., 2022), which resulted in faster
44 CO₂ removal due to photosynthesis than dissolution of CO₂ from the air (Stukel et al., 2023). It has
45 been assessed that, with the increasing anthropogenic CO₂ emissions, the oceanic CO₂ sink
46 increased from 1.7 ± 0.4 pg C yr⁻¹ in the 1980s to 2.5 ± 0.6 pg C yr⁻¹ in the 2010s (Friedlingstein
47 et al., 2025). Nevertheless, such apparent oceanic CO₂ uptake is altering carbonate chemistry in
48 surface oceans, leading to a pH drop of by 0.017–0.027 units per decade, with a potential further
49 drop by 0.3–0.4 units at the end of this century (Canadell et al., 2023; Gattuso et al., 2015). Such
50 progressive ocean acidification (OA) has been shown to impact many marine organisms (Gattuso et
51 al., 2015), including primary producers (Gao et al., 2020), subsequently feeding back on the CO₂
52 sequestration efficiency in marine systems including coastal waters.

53 OA in eutrophic coastal waters are suggested to progress faster than in open oceans by roughly
54 20 % due to CO₂ dissolution and enhanced remineralization of organic matters (Cai et al., 2011). The
55 subsequent changes in carbonate chemistry may thus drive shifts in phytoplankton community
56 structures/diversity and affect primary productions in differential ways due to regional
57 environmental traits and species-specific physiology (Feng et al., 2024; Gao et al., 2012). While the
58 effects of elevated pCO₂ on different phytoplankton assemblages have been demonstrated, positive,
59 neutral and negative effects have been reported, reflecting differences in experimental approaches
60 and/or phytoplankton compositions (Gao et al., 2020). Among the different approaches, field
61 mesocosm experiments under elevated pCO₂ projected for future OA scenario have been employed
62 to investigate the effects of OA on ecological processes, including primary production. ~~For example,~~
63 ~~mesocosm experiments showed that growth of coccolithophores was reduced~~ under 710 μatm pCO₂
64 during early summer in 2001 (Engel et al., 2005) and ~~their~~ ability to form blooms ~~disappeared~~ under
65 1000–3000 μatm pCO₂ during early summer in 2011 (Riebesell et al., 2017). Under elevated pCO₂,
66 ~~phytoplankton communities in Norwegian coastal mesocosms shifted from *Bathycoccus* to~~

删除了: These results indicate that the effects of OA on community structure can vary temporally and spatially.

删除了: Previous mesocosm experiments showed reduced growth of ...

删除了: growth species

删除了: the loss of

删除了: the

74 *Micromonas* (Meakin and Wyman, 2011). ~~In oligotrophic or mesotrophic conditions,~~ diatoms were
75 insensitive to OA, but ~~responded~~ positively under nutrient enrichment (Bach et al., 2019).
76 ~~Furthermore, nutrients enrichment also increased Chl *a* concentration under high *p*CO₂ condition~~
77 ~~(Riebesell et al., 2017; Tanaka et al., 2013; Schulz et al., 2013). By contrast, mesocosm experiments~~
78 ~~conducted in highly eutrophic water showed that high *p*CO₂ did not affect Chl *a* concentration (Liu~~
79 ~~et al., 2017).~~ Previously, we showed, by running a mesocosm experiment during spring of 2018 in
80 the southern coastal water of the East China Sea, that elevated *p*CO₂ of 1000 μatm suppressed the
81 succession from diatoms to dinoflagellates and increased the abundance of viruses and heterotrophic
82 bacteria, ~~promoting refueling of nutrients for phytoplankton growth (Huang et al., 2021). These~~
83 ~~findings indicate that plankton communities supported by nutrients from remineralization are more~~
84 sensitive to OA than those having access to higher availability of inorganic nutrients (Bach et al.,
85 2016; Bach et al., 2019). Overall, it is likely that ~~the effects of OA on community structure can vary~~
86 ~~temporally and spatially, and the~~ availabilities or levels of eutrophication can modulate the effects
87 of OA, alongside regional chemical and physical differences (Paul and Bach, 2020).

88 In coastal regions, changes in seawater carbonate chemistry influence primary production
89 which in reverse affect the pH change due to faster photosynthetic CO₂ removal than its dissolution
90 (Gao, 2021), resulting in increased pH during daytime and declined pH during nighttime. Such large
91 diel pH fluctuation may require phytoplankton to invest more energy to maintain cellular
92 homeostasis in response to the negative effects of increased hydrogen ion concentration (the acidic
93 stress), thereby affecting the functioning of planktonic ecosystem (Raven and Beardall, 2020;
94 Rokitta et al., 2012; Taylor et al., 2017). The ~~positive effects of increased inorganic carbon substrates~~
95 (e.g., CO₂ and HCO₃⁻) and the negative effect of increased H⁺ concentration may shape the
96 responses of coastal ecosystems to OA, leading to controversial results (Wu et al., 2017; Vázquez
97 et al., 2023; Chauhan et al., 2024). To better understand the consequences of OA in Chinese
98 eutrophic coastal regions, we conducted a mesocosm experiment in the eutrophic coastal water of
99 Wuyuan Bay, Xiamen, China, using *in situ* plankton communities during October-December, 2019
100 and investigated how OA shapes the diversity of phytoplankton community and affects primary
101 production processes. Our results show that in the eutrophic coastal water of East China Sea, with
102 the natural decrease of temperature, elevated *p*CO₂ increased primary production by promoting the

- 删除了: By contrast, another
- 删除了: mesocosm experiment carried out in
- 删除了: northeast Atlantic showing that
- 删除了: under oligotrophic conditions,
- 删除了: were
- 删除了: affected
- 移动了(插入) [1]
- 删除了: , however,
- 删除了: thereby
- 上移了 [2]: These results indicate that the effects of OA on community structure can vary temporally and spatially.
- 上移了 [1]: nutrients enrichment increased Chl *a* concentration under high *p*CO₂ condition (Riebesell et al., 2017; Tanaka et al., 2013; Schulz et al., 2013)
- 删除了: On the other hand, mesocosm experiments conducted in oligotrophic or mesotrophic regions showed that nutrients enrichment increased Chl *a* concentration under high *p*CO₂ condition (Riebesell et al., 2017; Tanaka et al., 2013; Schulz et al., 2013), however, mesocosm experiments conducted in highly eutrophic water showed that high *p*CO₂ did not affect Chl *a* concentration (Liu et al., 2017; Huang et al., 2021). ...P
- 删除了: P
- 删除了: remineralized
- 删除了: were
- 删除了: documented

130 phytoplankton biomass (indicated by Chl *a* concentration) under nutrient-replete condition, and
131 promoted smaller phytoplankton's growth to sustain the primary production after the nutrient
132 depletion and diatom bloom collapsed, though suppressed the emergence of dinoflagellates.

133 **2 Materials and methods**

134 **2.1 Mesocosms setup and sampling**

135 The *in situ* mesocosm experiment was conducted at the Facility for the Study of Ocean
136 Acidification Impacts of Xiamen University (FOANIC-XMU) located in the subtropical coastal
137 region Wuyuan Bay of southern East China Sea (24.52°N, 117.18°E) from 9th October (day 0
138 relative to algal inoculation) to 14th November, 2019. Nine cylindrical and transparent
139 thermoplastic polyurethane (TPU) mesocosm bags, each 3 m deep and 1.5 m in diameter, were filled
140 with approximately 3000 L of *in situ* seawater that had been prefiltered (MU801-4T, Midea, China,
141 pore size of 0.01 μm). The mesocosms were hooked to and secured within steel frames. Two $p\text{CO}_2$
142 treatments were established to investigate the effects of ocean acidification on the *in situ*
143 phytoplankton community: an ambient $p\text{CO}_2$ treatment (AC, 410 μatm ; 4 numbered bags) and a
144 high $p\text{CO}_2$ treatment representative of end-of-century projections (HC, 1,000 μatm ; 5 numbered
145 bags). To adjust CO_2 in seawater in the HC bags to the projected 1000 μatm in 2100s, approximately
146 11 L of CO_2 -saturated seawater was added to each HC bag. The AC and HC $p\text{CO}_2$ levels were
147 maintained by bubbling with ambient air and pre-mixed air- CO_2 (1000 $\mu\text{atm CO}_2$), respectively, at
148 a rate of 5 L min^{-1} using a CO_2 Enricher (CE-100B, Wuhan Ruihua Instrument & Equipment Ltd,
149 China). After the carbonate system had been stabilized (leveled pH), 720 L of *in situ* seawater were
150 filtered by a 180 μm mesh to exclude large zooplankton, and each mesocosm bag was inoculated
151 with 80 L of it to initiate the coastal microbial community. Samples were taken from each bag at a
152 depth of 0.5m at 9:00 a.m. by niskin bottles every 1–3 days for physical, chemical and biological
153 analysis.

154 **2.2 Measurement of environmental factors**

155 Solar light intensity was monitored every minute throughout the experimental period using a
156 real-time solar irradiance monitoring device (EKO, Japan). Salinity, temperature and pH in each
157 mesocosm were measured with a salinometer, a digital thermometer and a pH meter (Orino 2 STAR,
158 Thermo Scientific, U. S. A, calibrated with standard NBS buffer), respectively. Dissolved inorganic

159 carbon (DIC) was sampled and measured using an Environmental Water Analyzer (Ma et al., 2018),
160 and total alkalinity (TA) measured using an Automated Spectrophotometric Analyzer (Li et al.,
161 2013). Other seawater carbonate chemistry parameters were calculated with CO2SYS software with
162 known parameters of $p\text{CO}_2$, salinity, pH, temperature, and nutrient concentration.

163 Nutrient samples of each bag were filtered through cellulose acetate membrane (0.22 μm , 47
164 μm), and the filtrate was divided into 2 subsamples; one was stored at -20°C for the measurement
165 of $\text{NO}_3^- + \text{NO}_2^-$, PO_4^{3-} , and NH_4^+ ; another stored at 4°C for the measurement of SiO_3^{2-} .
166 Measurement of $\text{NO}_3^- + \text{NO}_2^-$, PO_4^{3-} , and SiO_3^{2-} concentration was conducted using an auto-
167 analyzer (AA3, Seal, Germany), NH_4^+ was measured with indophenol blue spectrophotometry using
168 a spectrophotometer (Tri-223, Spectrum, China) at 25°C . NO_2^- and NO_3^- were analyzed using the
169 copper-cadmium reduction method, the standard concentrations used for the $\text{NO}_2^- + \text{NO}_3^-$ calibration
170 curve were 0, 1.04, 2.08, 4.16, 10.4, 20.8, and 41.6 μM , and those for NO_2^- calibration curve were
171 0, 0.04, 0.08, 0.16, 0.4, 0.8, and 1.6 μM (Dai et al., 2008). PO_4^{3-} and SiO_3^{2-} were measured using
172 typical spectrophotometric method (Knap et al., 1994), and the calibration curves of both parameters
173 were prepared using standard concentrations of 0, 0.08, 0.16, 0.32, 0.8, 1.6, 3.2 μM and 0, 4, 8, 16,
174 40, 80, 160 μM , respectively.

删除了: 0.45 mm

175 2.3 Measurement of chlorophyll *a* and particle organic matters

176 Water samples of each mesocosm (100 – 1000 mL, depending on the biomass in the
177 mesocosms) were filtered onto GF/F filter (Whatman, United States) by suction filter with low
178 vacuum pressure (≤ 0.02 Mpa) and soaked in 5 mL pure methanol overnight. The extracts were
179 centrifuged at $8000 \times g$ and 4°C for 10 min, then the absorption spectra of supernatants from 400
180 to 800 nm were measured using a UV-VIS spectrophotometer (DU 800, Beckman, U. S. A). The
181 Chl *a* concentration was calculated according to the following equation (Ritchie, 2006):

$$182 \text{Chl } a (\mu\text{g } L^{-1}) = 16.29 \times (A_{665} - A_{750}) - 8.54 \times (A_{652} - A_{750})$$

183 where A_{750} , A_{665} , and A_{652} represents the absorbance of Chl *a* at wave length 750, 665, and
184 652 nm, respectively.

185 For the analysis of particulate organic carbon (POC) and nitrogen (PON) across two particle
186 size fractions, water samples of known volume were first filtered through a 20 μm mash to obtain
187 subsamples containing particle organic matters smaller than 20 μm . Particles larger than 20 μm

删除了: no more than

190 (retained on 20 µm mesh) were backwashed using an equal volume of prefiltered (0.22 µm) *in situ*
191 seawater, yielding in subsamples containing particulate organic matters larger than 20 µm. All
192 subsamples were then filtered on pre-combusted (450 °C, 6 h) GF/F filter (Whatman) and stored at
193 -20 °C until analysis. Before analyses, all filters were fumed over pure HCl for 12 h and dried at
194 60 °C to remove inorganic carbon, then packed in tin cups and measured with a CHNS elemental
195 analyzer (Vario EL cube Elementar, Germany).

196 **2.4 Net primary production and dark respiration**

197 Before sunrise, 120 mL of water samples from each mesocosm were collected and dispensed
198 into six 25 mL borosilicate bottles (three bottles for 12 h incubations, and three for 24 h incubations).
199 For each culture duration of each mesocosm, two bottles were illuminated under natural light and
200 one bottle was wrapped tightly in aluminum foil as a dark control. After incubation, cells were
201 filtered onto the GF/F filters (Whatman) under dim light and stored at -20 °C. Before measurement,
202 filters were placed individually in 20 mL scintillation vials and exposed to HCl fumes overnight,
203 dried at 60 °C for over 6 h to remove any unincorporated H¹⁴CO₃⁻. The incorporated ¹⁴C by algae
204 was counted with a liquid scintillation counter (Beckman, LS6500, Germany) in the presence of 5
205 mL scintillation cocktail (Hisafe 3, Perkin-Elmer, United States). Nighttime respiratory carbon loss
206 was calculated as the difference between carbon fixation over 12 h (daytime primary production)
207 and 24 h (daily net primary production).

208 **2.5 Determination of phytoplankton biomass and community structure**

209 Water samples (500–2000 mL) from each mesocosm were collected into polyethylene bottles
210 and fixed with 1.5 % **acidic** lugol's iodine. The samples were statically placed **for 2-3 days and**
211 concentrated into 50 mL subsamples in the centrifuge tube using siphons within 3 days, **then**,
212 examined with a microscopy (Nikon Eclipse Ns2) and a plankton counting chamber to assess
213 phytoplankton abundance and diversity based on the morphological characteristics as previous
214 described (Hasle and Syvertsen, 1997; Steidinger and Jangen, 1997; Yang and Liu, 2018). To
215 distinguish whether dinoflagellates are autotrophic or heterotrophic, we observed living algal cells
216 in the unstained water samples under the microscope for cell transparency and the presence of
217 chloroplasts.

218 **An** aliquot of 100 µL for each mesocosm was loaded onto a counting chamber for microscopic

删除了: in a constant temperature oven

删除了: vity

删除了: vity

删除了: . The concentrated subsamples were

删除了: , as shown in Fig. S9

删除了: For cell counts, a

225 enumeration. In each aliquot, the count was deemed valid only when the total number of cells
226 exceeded 200; otherwise, the subsample volume for microscopy was increased to achieve sufficient
227 counts. For samples collected during the exponential growth phase that exhibited excessively high
228 cell densities, appropriate dilution with 0.22 μm -filtered, sterilized seawater was performed prior
229 to counting (State Oceanic Administration 2005).

230 2.6 Statistical analyses

231 The data were all expressed by the mean and standard deviation (means \pm SD) and plotted by
232 Origin 2024. Independent-samples *t*-test was conducted to check the significant effects of increased
233 $p\text{CO}_2$ at the level of $p < 0.05$ using SPSS 19. To evaluate α -diversity, Shannon diversity index was
234 calculated based on the relative abundances of phytoplankton taxa using the estimate R and diversity
235 functions from the vegan package (version 2.6-4) in R (Version 4.2.2). Shannon index incorporates
236 both species diversity and evenness. Patterns of physiological parameters over time were
237 emphasizing using generalized additive models (GAMs) and constructed using the 'mgcv' package
238 in R to analyze changes in physiology through the experiment.

239 3 Results

240 3.1 Environmental changes in the mesocosms

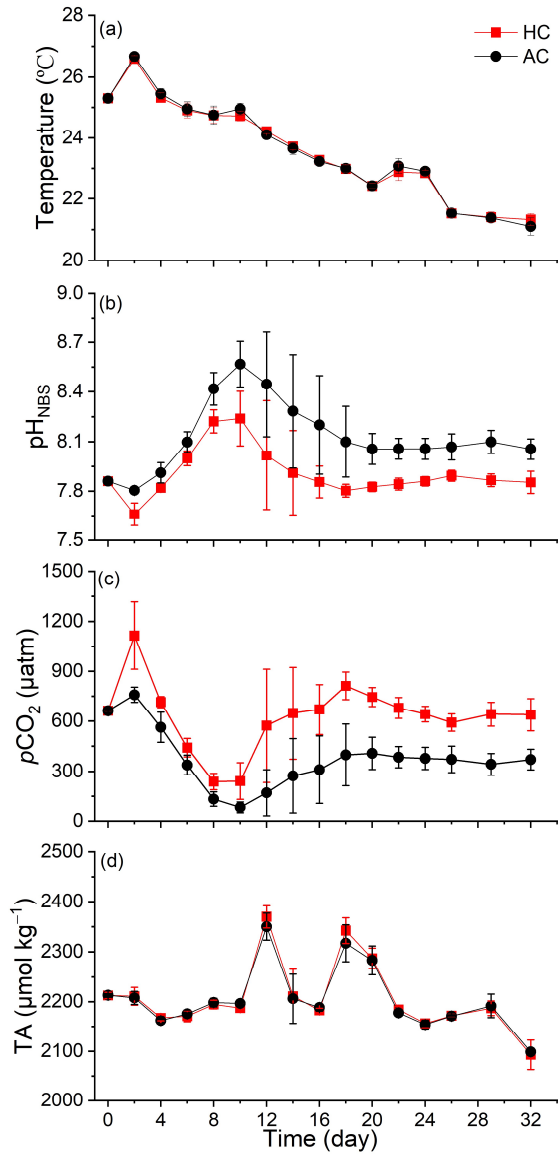
241 Throughout the experiment, most days were sunny, with daytime mean PAR (12h-average
242 photosynthetic active radiation) ranging from 200 to 850 $\mu\text{mol photons m}^{-2} \text{ s}^{-1}$ (Fig. S1). The
243 environmental temperatures decreased gradually from 26.7 ± 0.05 $^{\circ}\text{C}$ at day 0 (9th October) to 21.1
244 ± 0.28 $^{\circ}\text{C}$ at day 38 (14th November) (Fig. 1 a). Significant differences in pH_{NBS} and $p\text{CO}_2$ between
245 HC and AC were maintained throughout most of the experimental period, while there's no
246 significant difference in total alkalinity (TA) between the two $p\text{CO}_2$ treatments ($p = 4.02 \times 10^{-8}$,
247 2.87×10^{-12} , 0.549, respectively. Figs. 1 b-d, S5 a-c).

248 Following a sharp increase in phytoplankton biomass from day 4 to day 8 (Fig. 3 a), the pH_{NBS}
249 in the HC and AC mesocosms increased and peaked at 8.24 ± 0.16 and 8.56 ± 0.14 , respectively
250 (Fig. 1 b). Correspondingly, the $p\text{CO}_2$ value dropped to the lowest points of 238.48 ± 49.02 μatm
251 (HC) and 82.82 ± 32.88 μatm (AC) (Fig. 1 c). Then, as the phytoplankton biomass decreased after
252 day 8, pH_{NBS} gradually declined and $p\text{CO}_2$ increased, both stabilizing at relatively constant levels
253 from day 18 until the end of experiment. There were no obvious temporal changes observed in total

删除了: D

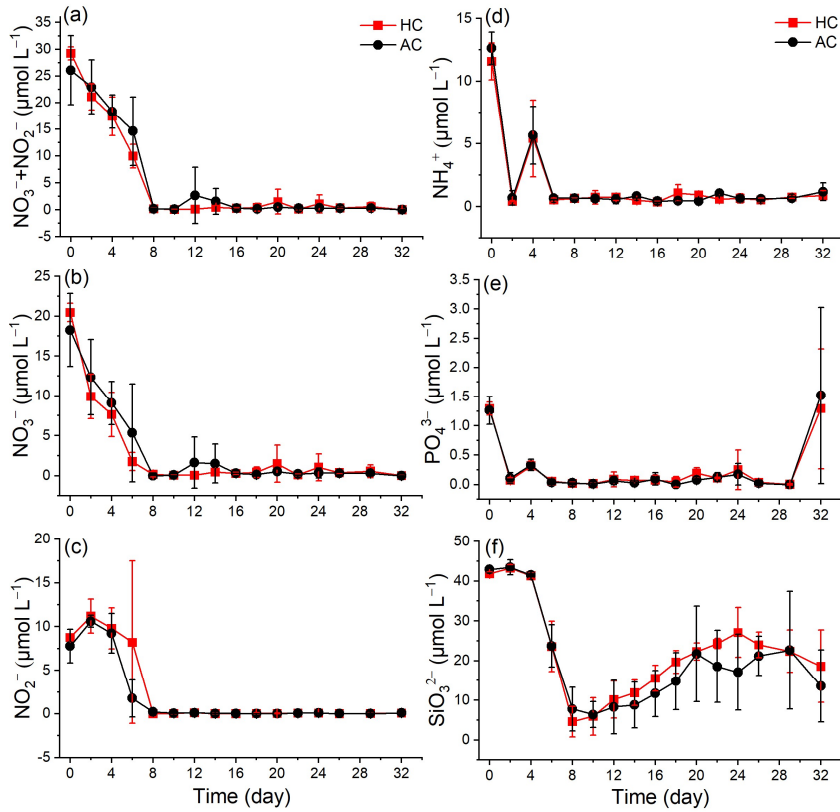
删除了: D

256 alkalinity (TA) throughout the experiment (Fig. 1 d).



257

258 Figure 1. Temporal variation of seawater temperature (a), pH_{NBS} (b), pCO₂ (c) and TA (d) in HC
259 (1000 µatm) and AC (410 µatm) mesocosms. The pCO₂ was estimated from the measured pH_{NBS}
260 and DIC concentration using the CO2SYS program. Data are means ± SD of 5 replicates for HC
261 and 4 replicates for AC mesocosms.



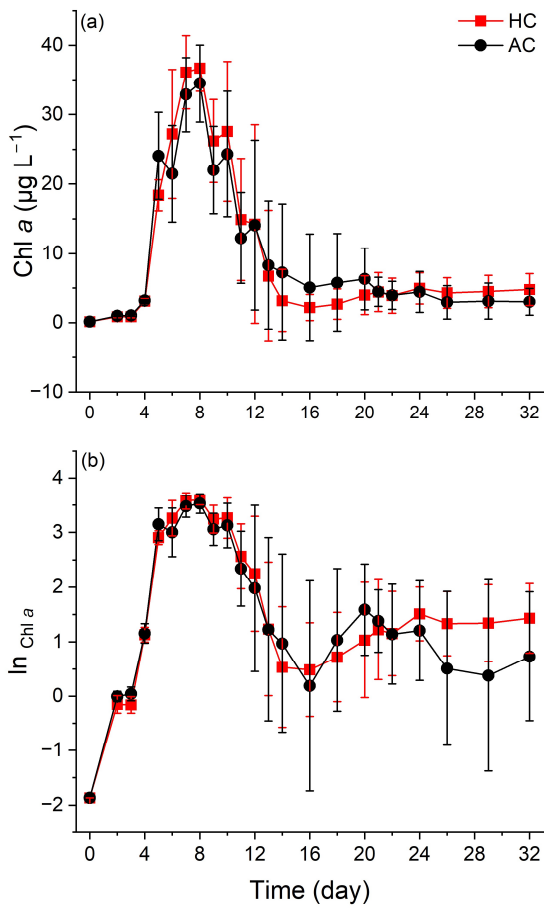
263

264 Figure 2. Temporal variation of nutrients (NO_3^- , NO_2^- , $\text{NO}_3^- + \text{NO}_2^-$, NH_4^+ , PO_4^{3-} , and SiO_3^{2-}) in
 265 HC (1000 μatm) and AC (410 μatm) mesocosms. Data are means \pm SD of 5 replicates for HC and
 266 4 replicates for AC mesocosms.

267

268 The initial nutrient concentrations reflected the eutrophic condition in the coastal seawater
 269 ($\text{NO}_3^- + \text{NO}_2^-$: 27 μM , PO_4^{3-} : 1.4 μM). In the mesocosm bags, nutrient concentrations declined
 270 dramatically in the early phase (up to day 8, Fig. 2). The $\text{NO}_3^- + \text{NO}_2^-$ and NO_3^- concentrations
 271 decreased sharply to nearly 0 by day 8 (Fig. 2 a, b). In contrast, the NO_2^- concentration experienced
 272 a slight increase on day 2, then declined to nearly 0 by day 8 and remained at a low level until the
 273 end of experiment in both HC and AC mesocosms (Fig. 2 c). Under HC condition, the NO_3^-

274 concentration decreased more rapidly than that under the AC until day 20, although the difference
 275 was not significant ($p = 0.423$, Fig. S5 d). Both NH_4^+ and PO_4^{3-} concentrations dropped to nearly 0
 276 after 4 days and remain relatively stable thereafter. There were no significant difference observed
 277 between HC and AC mesocosms ($p = 0.579$ and 0.631 , respectively, Figs. 2 d, e, S5 e, f). The SiO_3^{2-}
 278 concentration decreased from $41.81 \pm 0.48 \mu\text{M}$ in HC and $42.88 \pm 0.91 \mu\text{M}$ in AC on day 0 to a
 279 minimum of $4.62 \pm 3.82 \mu\text{M}$ and $7.79 \pm 5.52 \mu\text{M}$ by day 8, respectively. Thereafter, SiO_3^{2-}
 280 concentrations in both HC and AC mesocosms gradually increased until the end of experiment ($p =$
 281 0.343 , Figs. 2 f, S5 g).



282
 283 Figure 3. Temporal variations of Chl *a* concentration (a) and the LN scale of Chl *a* concentration (b)
 284 in HC (1000 μatm) and AC (410 μatm) mesocosms. Data are means \pm SD of 5 replicates for HC and

285 4 replicates for AC mesocosms.

286 **3.2 Chlorophyll *a* concentration**

287 Phytoplankton biomass, indirectly indicated by Chl *a* concentration, increased to peak at 35.88
288 $\pm 3.25 \mu\text{g L}^{-1}$ in the HC and 36.54 ± 4.88 in the AC mesocosms on day 8, and then gradually
289 decreased to $1.12 \pm 0.43 \mu\text{g L}^{-1}$ in HC by day 14 and $0.58 \pm 0.31 \mu\text{g L}^{-1}$ in AC by day 16, followed
290 by a slight increase by the end of experiment (Fig. 3 a). Based on the natural logarithm (ln) scale of
291 Chl *a* concentration, the phytoplankton growth kinetics under the two $p\text{CO}_2$ treatments showed the
292 following phases (Fig. 3 b): the exponential phase (from day 0 to day 5), the stationary phase (from
293 day 6 to day 10), the decline phase (from day 11 to day 16), and a second exponential phase from
294 day 17 to day 24 in the HC and to day 20 in the AC mesocosms. Then, phytoplankton assemblages
295 in the HC mesocosms entered a second stationary phase until the end of experiment, while in the
296 AC ones, they entered a decline phase until day 29, followed by a slight increase on day 32.

297 Throughout the experiment, the elevated $p\text{CO}_2$ resulted in higher average value of Chl *a*
298 concentration at most sampling times, although the differences were not statistically significant (p
299 $= 0.142$, Fig. S5 h).

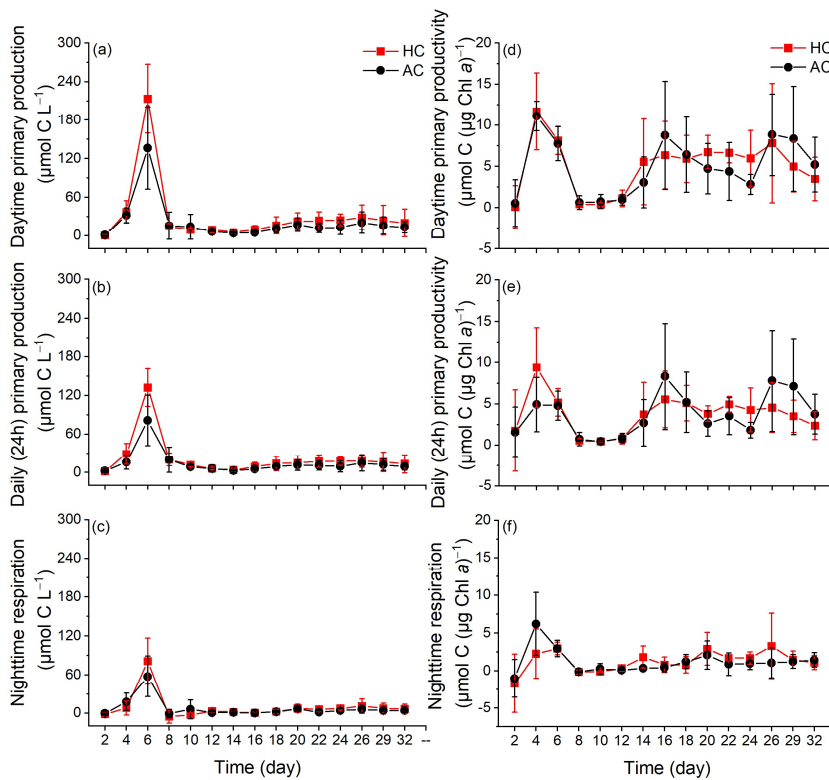
300 **3.3 Primary production and dark respiration**

301 The primary production and night-respiratory per water volume showed patterns similar to
302 those of phytoplankton biomass (indicated by Chl *a* concentration) (Fig. 4, a, b and c). They reached
303 their maximal values on day 6, which corresponded to the end of exponential phase. As the
304 phytoplankton communities entered the stationary phase, daytime (12 h) primary production, daily
305 (24 h) net primary production and nighttime respiration per water volume progressively decreased,
306 and then slightly increased again when the phytoplankton communities underwent the second
307 exponential phase. The elevated $p\text{CO}_2$ increased both daytime and daily net primary production
308 during the middle phase of the experiment, although the positive effect on 24 h primary production
309 tended to decline by the end of experiment ($p = 0.038$ and 0.012 , Fig. S6 a, b). The nighttime
310 respiration of phytoplankton was suppressed before day 8 and enhanced thereafter under the
311 elevated $p\text{CO}_2$, though no significant difference was observed ($p = 0.444$, Fig. S6 c).

312 Primary productivity per Chl *a* increased sharply on day 4, and decreased to the lowest values
313 on day 8. On day 12, both daytime and 24 h primary productivity in the HC increased drastically

314 and then remained relatively stable until the end of experiment (Fig. 4 d, e). In contrast, two
 315 additional peaks were observed in the AC mesocosms on days 16 and 26. The elevated $p\text{CO}_2$
 316 appeared to have enhanced primary productivity from day 2 to day 20, though these effects were
 317 not statistically significant ($p = 0.946$ for daytime and $p = 0.985$ for 24 h, Figs. 4 d, e, S6 d, e).

318 Nighttime respiration per μg Chl a initially increased on day 4, then decreased to nearly zero
 319 in both the HC and AC mesocosms on day 8 and remained relatively stable till the end of experiment.
 320 The elevated $p\text{CO}_2$ had a negative effect on phytoplankton respiration before day 12, but increased
 321 it thereafter, though no significant difference was observed between the HC and AC treatments ($p =$
 322 0.834 , Figs. 4 f, S6 f).



323
 324 Figure 4. The changes of daytime primary production (a) and primary productivity (b), daily (24h)
 325 primary production (c) and primary productivity (d), nighttime respiration per water volume (e) and
 326 per Chl a (f) in HC (1000 μatm) and AC (410 μatm) mesocosms. Data are means \pm SD of 5 replicates

327 for HC and 4 replicates for AC mesocosms.

328

329 3.4 Changes in Phytoplankton community and diversity

330 A total of 47 genera identified microscopically include 33 genera of diatoms, 7 of
331 dinoflagellates, 2 of cyanobacteria, 2 of chlorophyta, 2 of cryptophyta and 1 of euglenophyta. In all
332 mesocosms, the dominant species included *Cerataulina pelagica*, *Eucampia cornuta*, *Guinardia*
333 *delicatula*, *Leptocylindrus danicus*, *Skeletonema costatum*, *Protoperidinium* sp., *Gyrodinium*
334 *spirale*, *Cryptophyta* sp. and *Pyramimonas* sp. (Fig. S4).

335 Phytoplankton communities underwent dynamic succession in the mesocosms (Fig. 5).
336 Diatoms (mainly *Cerataulina pelagica*) dominated the phytoplankton communities during the early
337 and middle stages of the experiment, as indicated by the similar temporal trends in total
338 phytoplankton and diatom cell counts compared with Chl *a* concentration (Figs. 5 a, b, S4 a). ~~There~~
339 ~~was no significant difference in diatom density between the HC and AC mesocosms ($p = 0.259$, Fig.~~
340 ~~S7a), although the average value was lower in the former than in the latter treatment.~~ Autotrophic
341 dinoflagellates began to emerge on day 8 and rapidly declined on day 12 in both HC and AC
342 enclosures (Fig. 5 c). Except for days 6 to 18, the elevated $p\text{CO}_2$ increased the biomass of
343 autotrophic dinoflagellates, though the difference was insignificant ($p = 0.505$, Fig. S7 b). Hetero-
344 dinoflagellates began to emerge on day 6, with their abundance peaked on day 12 in the AC and on
345 day 14 in the HC mesocosms, then decreased by day 22. The elevated $p\text{CO}_2$ did not result in any
346 significant change in terms of their cell numbers ($p = 0.785$, Figs. 5 d, S7 c). On day 26, the biomass
347 of hetero-dinoflagellates increased again in the HC treatment, while it remained constant in the AC
348 treatment ($p = 0.729$, Independent-samples *t*-test).

349 The biomass of small taxa (Cyanobacteria, Chlorophyta, Cryptophyta and Euglenophyta)
350 started to increase on day 8, the HC treatment significantly increased the total biomass of these
351 small phytoplankton species thereafter ($p = 0.019$, Figs. 5 e, S4 h, i, S7 d). From day 22, when
352 diatoms biomass decreased to the lowest level, the temporal variation in small taxa biomass became
353 the main factor controlling overall phytoplankton dynamics (Figs. 5 e, S4 h, i). Accordingly, the
354 positive effect of HC on the small phytoplankton species led to an earlier transition of phytoplankton
355 from the large diatoms and dinoflagellate (mainly fall within the micro size fraction) to the smaller

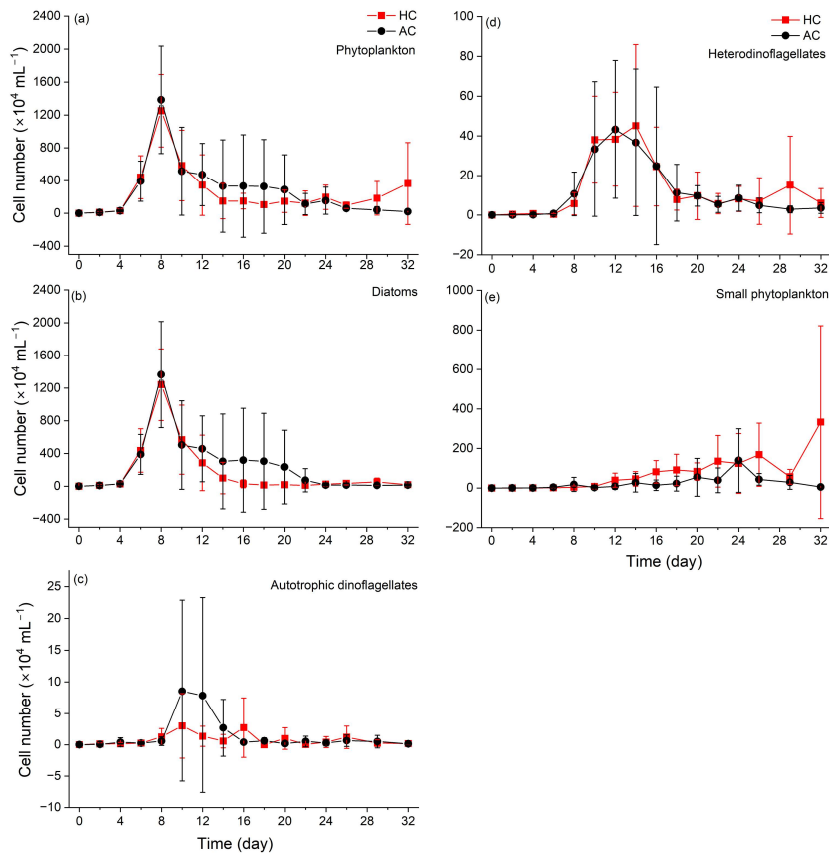
删除了: statistically

删除了: Diatom density was lower in the HC than in the AC mesocosms, though the difference was not statistically significant ($p = 0.259$, Fig. S7 a)

360 ones (Fig. 6 a, b). This accelerated transition in the HC treatment was also evidenced by higher
 361 concentration of POC and PON in the <20 μm fraction and lower concentration in the >20 μm
 362 fraction (Figs. S2, S3).

363 In both HC and AC mesocosms, Shannon diversity index decreased sharply from day 2,
 364 reaching the lowest values on day 8 in AC mesocosms and on day 10 in HC mesocosms (Fig. S8 a).
 365 Before day 22, Shannon diversity index increased under elevated $p\text{CO}_2$, whereas it is lowered under
 366 elevated $p\text{CO}_2$ level since day 24, although the differences were not statistically significant ($p =$
 367 0.161, Fig. S8 b).

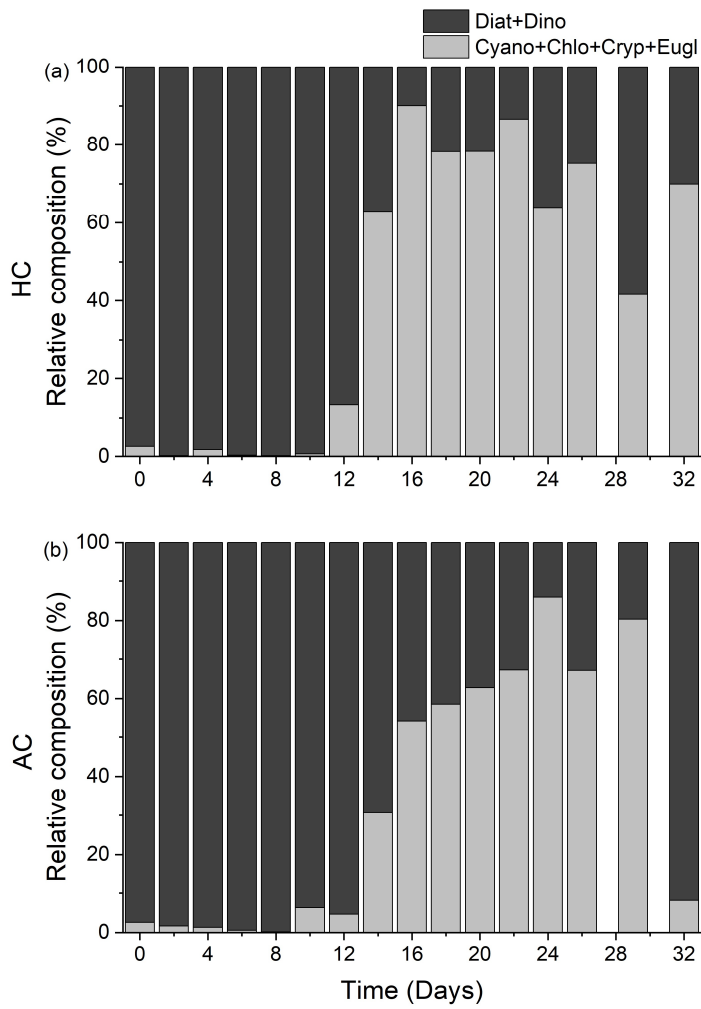
368



369
 370 Figure 5. Temporal variations of phytoplankton (a), diatoms (b), autotrophic dinoflagellates (c),
 371 heterodinoflagellates (d) and (e) small phytoplankton (Cyanobacteria, Chlorophyta, Cryptophyta

删除了: photo

373 and Euglenophyta) cell numbers in HC (1000 μatm) and AC (410 μatm) mesocosms. Data are means
 374 \pm SD of 5 replicates for HC and 4 replicates for AC mesocosms.



375
 376 Figure 6. Temporal variations of the relative composition of diatoms + dinoflagellates (Diat + Dino,
 377 black), Cyanobacteria + Chlorophyta + Cryptophytes + Euglenophyta (Cyano + Chlo + Cryp + Eugl,
 378 grey) in HC (1000 μatm , a) and AC (410 μatm , b) mesocosms. Data are means of 5 replicates for
 379 HC and 4 replicates for AC mesocosms.

380

381 **4 Discussion**

382 Ocean global changes have been suggested to alter community structure and reduce the
383 phytoplankton diversity due to physicochemical environmental changes (Henson et al., 2021; Yuan
384 et al., 2020). Specifically, there appears a growing trend of increasing dinoflagellates abundance
385 relative to diatoms (Carreto et al., 2018). Our mesocosm experiment, conducted in the highly
386 eutrophic Wuyuan Bay in the southern East China Sea during late autumn, also indicated that
387 elevated $p\text{CO}_2$, along with the natural decrease of surface water temperature and declined nutrient
388 availability, altered the structure and diversity of phytoplankton community. The diatom dominance
389 corresponded to the decreased diversity and evenness of phytoplankton community, while these
390 were recovered when the diatom dominance was replaced by dinoflagellates. However, this shift
391 from diatoms to autotrophic dinoflagellates was relatively suppressed under elevated $p\text{CO}_2$
392 conditions. In our mesocosms, the dinoflagellates that emerged during the mid-phase (e.g.,
393 *Protopteridinium* sp., *Pentaphtarsodinium dalei* and *Heterocapsa* sp., Fig. S9 a) were predominantly
394 small (<20 μm , Fig. S4 g) (Gu et al., 2013; Hanifah et al., 2022). but, these dinoflagellates were soon
395 replaced by an even smaller size fraction, including Cyanobacteria, Chlorophyta, Cryptophytes, and
396 Euglenophyta (Figs. 5, 6, S4). Ultimately, these smaller taxa maintained the primary production of
397 phytoplankton communities after nutrient depletion (Fig. 4).

398 When diatoms dominated the phytoplankton community (before day 8), primary production
399 per water volume and per μg Chl *a* did not change in the same pattern with increased diatom biomass
400 (Fig. 4). This is likely attributable to the larger size of photosynthetic unit (PSU) and lower reaction
401 center-to-Chl *a* ratio in diatoms, which could result in relatively lower photosynthetic efficiency
402 (Wu et al., 2014; Malerba et al., 2018). Meanwhile, The competitive advantages conferred by CO_2 -
403 concentrating mechanisms (CCMs) in diatoms led to insignificant lower biomass (Figs. 5 b, S7 a)
404 but higher primary production per water volume and per μg Chl *a* (Fig. 4 a, b, d and e) under elevated
405 $p\text{CO}_2$: their higher CO_2 affinity and CCMs plasticity may help diatoms gain a competitive advantage
406 in DIC uptake under ocean acidification scenarios (Huang et al., 2021; Raven and Beardall, 2020).
407 Furthermore, the down-regulated of CCMs in diatoms can save energy for other physiology
408 processes and thereby fuel their primary production (see the review by Gao and Campbell, 2014
409 and the references therein). These benefits resulting from elevated $p\text{CO}_2$ also led to higher diversity

删除了: diversity of

删除了: diversity and evenness

删除了: h

删除了: . Subsequently,

删除了: μg

删除了: when

删除了: increased

删除了: ,

删除了: which

删除了: size

删除了: may

删除了: elevated $p\text{CO}_2$ had an insignificant negative effect on their biomass (Figs. 5 b, S7 a), but increased the primary production per water volume and per μg Chl *a* (Fig. 4 a, b, d and e).

删除了: se may be attributed to the

删除了: level

427 and evenness (Fig. S8 a, b), suggesting that more diatom species were benefited from the elevated
428 $p\text{CO}_2$. While previous works have demonstrated a positive effect of elevated $p\text{CO}_2$ on the
429 photosynthetic carbon fixation by diatoms grown under low light and phytoplankton assemblages
430 in waters of higher nutrient availability (Gao et al., 2022), our results (Figs. 5 b, S1) indicate that
431 nutrient limitation can override or even reverse to the positive effects of elevated $p\text{CO}_2$ on diatoms
432 (Boyd et al., 2016; Li et al., 2018).

433 It appeared that dinoflagellates were less sensitive to the depletion of nutrients compared to
434 diatoms, with autotrophic dinoflagellates were more sensitive to elevated $p\text{CO}_2$ (Figs. 5 c, S7 b).
435 These suppressed transition from diatoms to autotrophic dinoflagellates under the elevated $p\text{CO}_2$
436 was consistent with our previous works, though conducted in different seasons (Huang et al., 2021),
437 which is likely due to the different CCMs efficiency and/or acidic resilience between dinoflagellates
438 and diatoms. Since the affinity of ribulose 1, 5-diphosphate carboxylase/oxidase (Rubisco) for CO_2
439 is much lower in autotrophic dinoflagellates than in diatoms (Reinfelder, 2011), elevated $p\text{CO}_2$ must
440 have benefitted the former more compared the latter, though invisible growth advantage was
441 observed on the autotrophic dinoflagellates between days 8 and 16. The heterodino­flagellates can
442 utilize organic matters (Glibert and Legrand, 2006) and prey on microbes including bacteria and
443 smaller microalgae (Jeong et al., 2010). This versatile nutrition strategy supported their rapid bloom
444 starting from day 8, leading to the replacement of autotrophic ones from day 12 onward (Fig. 5 c,
445 d). Although they were shown to be insensitive to ocean acidification (Meunier et al., 2017), their
446 respiration was depressed due to the acidic stress, raising their resilience in terms of energetic cost
447 (Wang and Gao, 2024). These mechanisms likely explain the observed insignificant effects of HC
448 on hetero-dino­flagellates.

449 The gradual increase in SiO_3^{2-} concentration, a nutrient exclusively required by diatoms,
450 coincided with their decline, confirming the low abundance of diatoms in the mid and late phase of
451 experiment, while the slightly increases in $\text{NO}_3^- + \text{NO}_2^-$, PO_4^{3-} and SiO_3^{2-} concentrations from day
452 10 onward (Fig. 2 a, e, f) should be attributed to remineralization by heterotrophic bacteria
453 (Aristegui et al., 2009; Bunse and Pinhassi, 2017). These regenerated $\text{NO}_3^- + \text{NO}_2^-$ and PO_4^{3-}
454 subsequently refueled the growth of small phytoplankton taxa, recover the diversity and evenness
455 in the phytoplankton communities (Figs. 5 e, S8 a, b) (Thingstad and Rassoulzadegan, 1995).

删除了: , though the total diatom biomass was lower in HC mesocosms (Figs. S4, S7 a)

移动了(插入) [3]

删除了: T

上移了 [3]: The gradual increase in SiO_3^{2-} concentration, a nutrient exclusively required by diatoms, coincided with their decline, confirming the low abundance of diatoms in the mid and late phase of experiment.

463 Alternatively, it is plausible that grazing activity by zooplankton, which was not quantified in this
464 study, also contributed to the apparent rise in diversity and evenness, as grazers tend to consume
465 dominant phytoplankton taxa (Thingstad and Rassoulzadegan, 1999; Calbet and Landry, 2004).

466 The dominant small taxa, such as *Cryptophyta* sp. and green microalga *Pyramimonas* sp. (Fig.
467 S4 h, i) during days 16–24, achieved primary productivity (per $\mu\text{g Chl } a$) comparable to the diatom-
468 dominated community observed on days 4–6 (Fig. 4 b, d). The success of these small taxa after
469 nutrient depletion can be attributed to their small size and larger surface-to-volume ratio (Finkel et
470 al., 2009; Giordano et al., 2005), which might enable them with higher efficiency in nutrients uptake
471 and CO_2 diffusion. Furthermore, the higher abundance of viruses and heterotrophic bacteria in the
472 HC mesocosms (Huang et al., 2021; Lin et al., 2018) intensified nutrient remineralization,
473 subsidizing these small, fast-growing phototrophs and leading to their earlier emergence on day 16
474 compared to day 24 in the AC mesocosms (Fig. 6). While it's possible that picophytoplankton
475 originally present in this region (Zhong et al., 2020) were missed by microscope-based identification,
476 it is reasonable to infer that they also contributed to the late-phase primary production. Previous
477 studies indicated that, after diatom/dinoflagella blooms and nutrient depletion, remineralized
478 nutrients in the seawater may also favor the growth of picophytoplankton (Nishibe et al., 2015; Fu
479 et al., 2009) and elevated $p\text{CO}_2$ would further benefit their growth. Thus, it is likely that,
480 picophytoplankton also dominated the phytoplankton communities in the HC mesocosms.

481 Though previous studies have suggested the changing temperatures influenced the
482 phytoplankton growth and community structure individually or interactively, with OA and other
483 environmental factors (Bénard et al., 2018; Courboulès et al., 2018; Li et al., 2018), the results from
484 the present autumn mesocosm experiment revealed the same pattern with our previous spring
485 mesocosm experiment (Huang et al., 2021), suggesting that it is not the seasonal temperature
486 trajectories but the availability of nutrients that controlled the shift from diatom to dinoflagellate
487 dominance, leading to declines in primary productivity (Huang et al., 2021; Cloern, 1996). Such
488 consistency underscores that nutrient availability and stoichiometry are the primary determinants of
489 phytoplankton community composition, usually exerting stronger and more immediate effects on
490 taxonomic and functional group dominance (Karl et al., 1996; Paerl and Paul, 2012; Ptacnik et al.,
491 2008; Meyer et al., 2016), though thermal and acidic stresses can impact phytoplankton

删除了: in our mesocosm experiment

删除了: phytoplankton communities

删除了: Previous studies have suggested that the shift from diatom to dinoflagellate dominance was generally associated with declines in primary productivity (Huang et al., 2021; Cloern, 1996).

删除了: in

删除了: ion

删除了: T

删除了: s

删除了: the

删除了: indicating

504 photosynthesis and respiration to greater extent under nutrient limitation (Li et al., 2018; Gao et al.,
505 2022).

506 Reduced nutrient availability usually decreases phytoplankton community richness (Gazeau et
507 al., 2017), although ocean acidification appeared to partly offset such effects (Fig. S8). However,
508 these compensatory effects diminished once both the initial and regenerated nitrogen sources were
509 exhausted (after day 24, Fig. S8 b). At that point, only a few small phytoplankton taxa tolerant to
510 low pH remained dominant, indicating a loss of diversity in the community and less stable
511 ecosystems (McCann, 2000) under combination of acidic stress and nutrient limitation. [In summary,](#)
512 [beyond compensating previous works, our study further demonstrated that progressive ocean](#)
513 [acidification is likely to reduce primary production, and phytoplankton diversity in the eutrophicated](#)
514 coastal water of the southern East China Sea.

删除了: vity

515 **Data availability Statement**

516 All relevant data are presented in the paper and its Supporting Information file, and will be available
517 upon request to the corresponding author Kunshan Gao.

518 **Conflict of Interest**

519 The authors declare no competing interests.

520 **Acknowledgements**

521 This study was supported by the National Key Research and Development Program of China
522 (2022YFC3105303), the National Natural Science Foundation of China (42361144840,
523 41720104005). We are grateful to the engineers, Xianglan Zeng and Wenyan Zhao, for their
524 technical supports, and we thank Prof. Jian Ma (College of the Environment and Ecology, Xiamen
525 University) for providing the Environmental Water Analyzer (iSEA) during the mesocosm
526 experiment.

527 **Author's Contributions**

528 Kunshan Gao and Guang Gao designed the mesocosm experiment; Yuming Rao, Na Wang, Jiazhen
529 Sun, Xiaowen Jiang, Di Zhang, Liming Qu, He Li, Qianqian Fu, Xuyang Wang, Cong Zhou, Zichao
530 Deng, Yang Tian, Xiangqi Yi, Ruiping Huang performed the mesocosm experiment; Yuming Rao
531 analyzed the data and wrote up the manuscript; Na Wang performed microscopy observation;
532 Kunshan Gao edited the manuscript; All authors reviewed and contributed to revision of the

534 manuscript.

535

536 **References**

537 Arístegui, J., Gasol, J. M., Duarte, C. M., and Herndl, G. J.: Microbial oceanography of the dark ocean's
538 pelagic realm, *Limnol. Oceanogr.*, 54, 1501-1529, <https://doi.org/10.4319/lo.2009.54.5.1501>, 2009.

539 Bach, L. T., Hernández-Hernández, N., Taucher, J., Spisla, C., Sforna, C., Riebesell, U., and Arístegui,
540 J.: Effects of Elevated CO₂ on a Natural Diatom Community in the Subtropical NE Atlantic, *Front.
541 Mar. Sci.*, Volume 6 - 2019, 10.3389/fmars.2019.00075, 2019.

542 Bach, L. T., Taucher, J., Boxhammer, T., Ludwig, A., The Kristineberg, K. C., Achterberg, E. P., Alguero-
543 Muñoz, M., Anderson, L. G., Bellworthy, J., Büdenbender, J., Czerny, J., Ericson, Y., Esposito, M.,
544 Fischer, M., Haunost, M., Helleman, D., Horn, H. G., Hornick, T., Meyer, J., Sswat, M., Zark, M.,
545 and Riebesell, U.: Influence of Ocean Acidification on a Natural Winter-to-Summer Plankton
546 Succession: First Insights from a Long-Term Mesocosm Study Draw Attention to Periods of Low
547 Nutrient Concentrations, *Plos One*, 11, e0159068, 10.1371/journal.pone.0159068, 2016.

548 [Bénard, R., Levasseur, M., Scarratt, M., Blais, M. A., Mucci, A., Ferreyra, G., Starr, M., Gosselin, M.,
549 Tremblay, J. É., and Lizotte, M.: Experimental assessment of the sensitivity of an estuarine
550 phytoplankton fall bloom to acidification and warming, *Biogeosciences*, 15, 4883-4904,
551 \[10.5194/bg-15-4883-2018\]\(https://doi.org/10.5194/bg-15-4883-2018\), 2018.](#)

552 Boyd, P. W., Dillingham, P. W., McGraw, C. M., Armstrong, E. A., Cornwall, C. E., Feng, Y. y., Hurd, C.
553 L., Gault-Ringold, M., Roleda, M. Y., Timmins-Schiffman, E., and Nunn, B. L.: Physiological
554 responses of a Southern Ocean diatom to complex future ocean conditions, *Nat. Clim. Change.*, 6,
555 207-213, 10.1038/nclimate2811, 2016.

556 Bunse, C. and Pinhassi, J.: Marine Bacterioplankton Seasonal Succession Dynamics, *Trends. Microbiol.*,
557 25, 494-505, <https://doi.org/10.1016/j.tim.2016.12.013>, 2017.

558 Cai, W.-J., Hu, X., Huang, W.-J., Murrell, M. C., Lehrter, J. C., Lohrenz, S. E., Chou, W.-C., Zhai, W.,
559 Hollibaugh, J. T., and Wang, Y.: Acidification of subsurface coastal waters enhanced by
560 eutrophication, *Nat. Geosci.*, 4, 766-770, 2011.

561 Calbet, A. and Landry, M. R.: Phytoplankton growth, microzooplankton grazing, and carbon cycling in
562 marine systems, *Limnol. Oceanogr.*, 49, 51-57, <https://doi.org/10.4319/lo.2004.49.1.0051>, 2004.

563 Canadell, J. G., Monteiro, P. M., Costa, M. H., Cotrim da Cunha, L., Cox, P. M., Eliseev, A. V., Henson,
564 S., Ishii, M., Jaccard, S., and Koven, C.: Intergovernmental Panel on Climate Change (IPCC).
565 Global carbon and other biogeochemical cycles and feedbacks, in: Climate change 2021: The
566 physical science basis. Contribution of working group I to the sixth assessment report of the
567 intergovernmental panel on climate change, Cambridge University Press, 673-816, 2023.

568 Carreto, J. I., Carignan, M. O., Montoya, N. G., Cozzolino, E., and Akselman, R.: Mycosporine-like
569 amino acids and xanthophyll-cycle pigments favour a massive spring bloom development of the
570 dinoflagellate *Prorocentrum minimum* in Grande Bay (Argentina), an ozone hole affected area, *J.*
571 *Marine. Syst.*, 178, 15-28, <https://doi.org/10.1016/j.jmarsys.2017.10.004>, 2018.

572 Chauhan, N., Dedman, C. J., Baldreki, C., Dowle, A. A., Larson, T. R., and Rickaby, R. E. M.: Contrasting
573 species-specific stress response to environmental pH determines the fate of coccolithophores in
574 future oceans, *Mar. Pollut. Bull.*, 209, 117136, <https://doi.org/10.1016/j.marpolbul.2024.117136>,
575 2024.

576 Cloern, J. E.: Phytoplankton bloom dynamics in coastal ecosystems: A review with some general lessons
577 from sustained investigation of San Francisco Bay, California, *Rev. Geophys.*, 34, 127-168,
578 <https://doi.org/10.1029/96RG00986>, 1996.

579 [Courboulès, J., Vidussi, F., Soulié, T., Mas, S., Pecqueur, D., and Mostajir, B.: Effects of experimental](#)
580 [warming on small phytoplankton, bacteria and viruses in autumn in the Mediterranean coastal Thau](#)
581 [Lagoon, *Aquatic Ecology*, 55, 647-666, 10.1007/s10452-021-09852-7, 2021.](#)

582 [Dai, M., Wang, L., Guo, X., Zhai, W., Li, Q., He, B., and Kao, S. J.: Nitrification and inorganic nitrogen](#)
583 [distribution in a large perturbed river/estuarine system: the Pearl River Estuary, China,](#)
584 [*Biogeosciences*, 5, 1227-1244, 10.5194/bg-5-1227-2008, 2008.](#)

585 Engel, A., Zondervan, I., Aerts, K., Beaufort, L., Benthien, A., Chou, L., Delille, B., Gattuso, J.-P., Harlay,
586 J., and Heemann, C.: Testing the direct effect of CO₂ concentration on a bloom of the
587 coccolithophorid *Emiliania huxleyi* in mesocosm experiments, *Limnol. Oceanogr.*, 50, 493-507,
588 2005.

589 Feng, Y., Xiong, Y., Hall-Spencer, J. M., Liu, K., Beardall, J., Gao, K., Ge, J., Xu, J., and Gao, G.: Shift
590 in algal blooms from micro- to macroalgae around China with increasing eutrophication and climate
591 change, *Global Change Biol.*, 30, e17018, <https://doi.org/10.1111/gcb.17018>, 2024.

592 Finkel, Z. V., Beardall, J., Flynn, K. J., Quigg, A., Rees, T. A. V., and Raven, J. A.: Phytoplankton in a
593 changing world: cell size and elemental stoichiometry, *J. Plankton. Res.*, 32, 119-137,
594 10.1093/plankt/fbp098, 2009.

595 Friedlingstein, P., O'Sullivan, M., Jones, M. W., Andrew, R. M., Hauck, J., Landschützer, P., Le Quéré,
596 C., Li, H., Luijkx, I. T., Olsen, A., Peters, G. P., Peters, W., Pongratz, J., Schwingshackl, C., Sitch,
597 S., Canadell, J. G., Ciais, P., Jackson, R. B., Alin, S. R., Arneth, A., Arora, V., Bates, N. R., Becker,
598 M., Bellouin, N., Berghoff, C. F., Bittig, H. C., Bopp, L., Cadule, P., Campbell, K., Chamberlain,
599 M. A., Chandra, N., Chevallier, F., Chini, L. P., Colligan, T., Decayeux, J., Djeutchouang, L. M.,
600 Dou, X., Duran Rojas, C., Enyo, K., Evans, W., Fay, A. R., Feely, R. A., Ford, D. J., Foster, A.,
601 Gasser, T., Gehlen, M., Gkritzalis, T., Grassi, G., Gregor, L., Gruber, N., Gürses, Ö., Harris, I.,
602 Hefner, M., Heinke, J., Hurtt, G. C., Iida, Y., Ilyina, T., Jacobson, A. R., Jain, A. K., Jarníková, T.,
603 Jersild, A., Jiang, F., Jin, Z., Kato, E., Keeling, R. F., Klein Goldewijk, K., Knauer, J., Korsbakken,
604 J. I., Lan, X., Lauvset, S. K., Lefèvre, N., Liu, Z., Liu, J., Ma, L., Maksyutov, S., Marland, G., Mayot,
605 N., McGuire, P. C., Metzl, N., Monacci, N. M., Morgan, E. J., Nakaoka, S. I., Neill, C., Niwa, Y.,
606 Nützel, T., Olivier, L., Ono, T., Palmer, P. I., Pierrot, D., Qin, Z., Resplandy, L., Roobaert, A., Rosan,
607 T. M., Rödenbeck, C., Schwinger, J., Smallman, T. L., Smith, S. M., Sospedra-Alfonso, R., Steinhoff,
608 T., Sun, Q., Sutton, A. J., Séférian, R., Takao, S., Tatebe, H., Tian, H., Tilbrook, B., Torres, O.,
609 Tourigny, E., Tsujino, H., Tubiello, F., van der Werf, G., Wanninkhof, R., Wang, X., Yang, D., Yang,
610 X., Yu, Z., Yuan, W., Yue, X., Zaehle, S., Zeng, N., and Zeng, J.: Global Carbon Budget 2024, *Earth*
611 *Syst. Sci. Data*, 17, 965-1039, 10.5194/essd-17-965-2025, 2025.

612 Fu, M., Wang, Z., Li, Y., Li, R., Sun, P., Wei, X., Lin, X., and Guo, J.: Phytoplankton biomass size
613 structure and its regulation in the Southern Yellow Sea (China): Seasonal variability, *Cont. Shelf*
614 *Res.*, 29, 2178-2194, <https://doi.org/10.1016/j.csr.2009.08.010>, 2009.

615 Gao, K.: Approaches and involved principles to control pH/pCO₂ stability in algal cultures, *J. Appl.*
616 *Phycol.*, 33, 3497-3505, 2021.

617 Gao, K. and Campbell, D. A.: Photophysiological responses of marine diatoms to elevated CO₂ and
618 decreased pH: a review, *Funct. Plant. Biol.*, 41, 449-459, <https://doi.org/10.1071/FP13247>, 2014.

619 Gao, K., Zhao, W., and Beardall, J.: Future responses of marine primary producers to environmental
620 changes, *Blue Planet, Red and Green Photosynthesis: Productivity and Carbon Cycling in Aquatic*

621 Ecosystems, 273-304, 2022.

622 Gao, K., Gao, G., Wang, Y., and Dupont, S.: Impacts of ocean acidification under multiple stressors on
623 typical organisms and ecological processes, *Mar. Life. Sci. Tech.*, 2, 279-291, 2020.

624 Gao, K., Xu, J., Gao, G., Li, Y., Hutchins, D. A., Huang, B., Wang, L., Zheng, Y., Jin, P., and Cai, X.:
625 Rising CO₂ and increased light exposure synergistically reduce marine primary productivity, *Nat.*
626 *Clim. Change.*, 2, 519-523, 2012.

627 Gattuso, J.-P., Magnan, A., Billé, R., Cheung, W. W., Howes, E. L., Joos, F., Allemand, D., Bopp, L.,
628 Cooley, S. R., and Eakin, C. M.: Contrasting futures for ocean and society from different
629 anthropogenic CO₂ emissions scenarios, *Science*, 349, aac4722, 2015.

630 Gazeau, F., Sallon, A., Pitta, P., Tsiola, A., Maugendre, L., Giani, M., Celussi, M., Pedrotti, M. L., Marro,
631 S., and Guieu, C.: Limited impact of ocean acidification on phytoplankton community structure and
632 carbon export in an oligotrophic environment: Results from two short-term mesocosm studies in the
633 Mediterranean Sea, *Estuar. Coast. Shelf. S.*, 186, 72-88, <https://doi.org/10.1016/j.ecss.2016.11.016>,
634 2017.

635 Giordano, M., Norici, A., and Hell, R.: Sulfur and phytoplankton: acquisition, metabolism and impact on
636 the environment, *New. Phytol.*, 166, 371-382, 2005.

637 Glibert, P. M. and Legrand, C.: The Diverse Nutrient Strategies of Harmful Algae: Focus on Osmotrophy,
638 in: *Ecology of Harmful Algae*, edited by: Granéli, E., and Turner, J. T., Springer Berlin Heidelberg,
639 Berlin, Heidelberg, 163-175, 10.1007/978-3-540-32210-8_13, 2006.

640 Gu, H., Luo, Z., Zeng, N., Lan, B., and Lan, D.: First record of *Pentapharsodinium* (Peridinales,
641 Dinophyceae) in the China Sea, with description of *Pentapharsodinium dalei* var. *aciculiferum*,
642 *Phycological Research*, 61, 256-267, <https://doi.org/10.1111/pre.12024>, 2013.

643 Hanifah, A. H., Teng, S. T., Law, I. K., Abdullah, N., Chiba, S. U. A., Lum, W. M., Tillmann, U., Lim, P.
644 T., and Leaw, C. P.: Six marine thecate *Heterocapsa* (Dinophyceae) from Malaysia, including the
645 description of three novel species and their cytotoxicity potential, *Harmful. algae.*, 120, 102338,
646 <https://doi.org/10.1016/j.hal.2022.102338>, 2022.

647 Hasle, G. R. and Syvertsen, E. E.: Chapter 2 - Marine Diatoms, in: *Identifying Marine Phytoplankton*,
648 edited by: Tomas, C. R., Academic Press, San Diego, 5-385, [https://doi.org/10.1016/B978-](https://doi.org/10.1016/B978-012693018-4/50004-5)
649 [012693018-4/50004-5](https://doi.org/10.1016/B978-012693018-4/50004-5), 1997.

650 Henson, S. A., Cael, B. B., Allen, S. R., and Dutkiewicz, S.: Future phytoplankton diversity in a changing
651 climate, *Nat. Commun.*, 12, 5372, 10.1038/s41467-021-25699-w, 2021.

652 Huang, R., Sun, J., Yang, Y., Jiang, X., Wang, Z., Song, X., Wang, T., Zhang, D., Li, H., and Yi, X.:
653 Elevated $p\text{CO}_2$ Impedes Succession of Phytoplankton Community From Diatoms to Dinoflagellates
654 Along With Increased Abundance of Viruses and Bacteria, *Front. Mar. Sci.*, 8, 642208, 2021.

655 Jeong, H. J., Yoo, Y. D., Kim, J. S., Seong, K. A., Kang, N. S., and Kim, T. H.: Growth, feeding and
656 ecological roles of the mixotrophic and heterotrophic dinoflagellates in marine planktonic food
657 webs, *Ocean. Sci. J.*, 45, 65-91, 10.1007/s12601-010-0007-2, 2010.

658 Karl, D. M., Christian, J. R., Dore, J. E., Hebel, D. V., Letelier, R. M., Tupas, L. M., and Winn, C. D.:
659 Seasonal and interannual variability in primary production and particle flux at Station ALOHA,
660 *Deep-Sea. Res. Pt. II*, 43, 539-568, [https://doi.org/10.1016/0967-0645\(96\)00002-1](https://doi.org/10.1016/0967-0645(96)00002-1), 1996.

661 [Knap, A., Michaels, A., Close, A., Ducklow, H., and Dickson, A.: Protocols for the Joint Global Ocean](#)
662 [Flux Study \(JGOFS\) core measurements, vi+170 pp.1994.](#)

663 Li, F., Beardall, J., and Gao, K.: Diatom performance in a future ocean: interactions between nitrogen
664 limitation, temperature, and CO_2 -induced seawater acidification, *ICES. J. Mar. Sci.*, 75, 1451-1464,
665 10.1093/icesjms/fsx239, 2018.

666 Li, Q., Wang, F., Wang, Z. A., Yuan, D., Dai, M., Chen, J., Dai, J., and Hoering, K. A.: Automated
667 Spectrophotometric Analyzer for Rapid Single-Point Titration of Seawater Total Alkalinity, *Environ.*
668 *Sci. Technol.*, 47, 11139-11146, 10.1021/es402421a, 2013.

669 Lin, X., Huang, R., Li, Y., Li, F., Wu, Y., Hutchins, D. A., Dai, M., and Gao, K.: Interactive network
670 configuration maintains bacterioplankton community structure under elevated CO_2 in a eutrophic
671 coastal mesocosm experiment, *Biogeosciences*, 15, 551-565, 10.5194/bg-15-551-2018, 2018.

672 Liu, N., Tong, S., Yi, X., Li, Y., Li, Z., Miao, H., Wang, T., Li, F., Yan, D., Huang, R., Wu, Y., Hutchins,
673 D. A., Beardall, J., Dai, M., and Gao, K.: Carbon assimilation and losses during an ocean
674 acidification mesocosm experiment, with special reference to algal blooms, *Mar. Environ. Res.*, 129,
675 229-235, <https://doi.org/10.1016/j.marenvres.2017.05.003>, 2017.

676 Ma, J., Li, P., Chen, Z., Lin, K., Chen, N., Jiang, Y., Chen, J., Huang, B., and Yuan, D.: Development of
677 an Integrated Syringe-Pump-Based Environmental-Water Analyzer (iSEA) and Application of It for
678 Fully Automated Real-Time Determination of Ammonium in Fresh Water, *Anal. Chem.*, 90, 6431-

679 6435, 10.1021/acs.analchem.8b01490, 2018.

680 McCann, K. S.: The diversity–stability debate, *Nature*, 405, 228-233, 10.1038/35012234, 2000.

681 Meakin, N. G. and Wyman, M.: Rapid shifts in picoeukaryote community structure in response to ocean
682 acidification, *ISME J.*, 5, 1397-1405, 10.1038/ismej.2011.18, 2011.

683 Meunier, C. L., Algueró-Muñiz, M., Horn, H. G., Lange, J. A. F., and Boersma, M.: Direct and indirect
684 effects of near-future CO₂ levels on zooplankton dynamics, *Mar. Freshwater. Res.*, 68, 373-380,
685 <https://doi.org/10.1071/MF15296>, 2017.

686 Meyer, J., Löscher, C. R., Neulinger, S. C., Reichel, A. F., Loginova, A., Borchard, C., Schmitz, R. A.,
687 Hauss, H., Kiko, R., and Riebesell, U.: Changing nutrient stoichiometry affects phytoplankton
688 production, DOP accumulation and dinitrogen fixation – a mesocosm experiment in the eastern
689 tropical North Atlantic, *Biogeosciences*, 13, 781-794, 10.5194/bg-13-781-2016, 2016.

690 Nishibe, Y., Takahashi, K., Shiozaki, T., Kakehi, S., Saito, H., and Furuya, K.: Size-fractionated primary
691 production in the Kuroshio Extension and adjacent regions in spring, *J. Oceanogr.*, 71, 27-40,
692 10.1007/s10872-014-0258-0, 2015.

693 Paerl, H. W. and Paul, V. J.: Climate change: Links to global expansion of harmful cyanobacteria, *Water*.
694 *Res.*, 46, 1349-1363, <https://doi.org/10.1016/j.watres.2011.08.002>, 2012.

695 Paul, A. J. and Bach, L. T.: Universal response pattern of phytoplankton growth rates to increasing CO₂,
696 *New. Phytol.*, 228, 1710-1716, <https://doi.org/10.1111/nph.16806>, 2020.

697 Ptacnik, R., Solimini, A. G., Andersen, T., Tamminen, T., Brettum, P., Lepistö, L., Willén, E., and
698 Rekolainen, S.: Diversity predicts stability and resource use efficiency in natural phytoplankton
699 communities, *Proc. Natl. Acad. Sci.*, 105, 5134-5138, doi:10.1073/pnas.0708328105, 2008.

700 Raven, J. A. and Beardall, J.: Energizing the plasmalemma of marine photosynthetic organisms: the role
701 of primary active transport, *J. Mar. Biol. Assoc. Uk.*, 100, 333-346, 2020.

702 Reinfelder, J. R.: Carbon concentrating mechanisms in eukaryotic marine phytoplankton, *Annu. Rev.*
703 *Mar. Sci.*, 3, 291-315, 2011.

704 Riebesell, U., Bach, L. T., Bellerby, R. G., Monsalve, J. R. B., Boxhammer, T., Czerny, J., Larsen, A.,
705 Ludwig, A., and Schulz, K. G.: Competitive fitness of a predominant pelagic calcifier impaired by
706 ocean acidification, *Nat. Geosci.*, 10, 19-23, 2017.

707 Ritchie, R. J.: Consistent sets of spectrophotometric chlorophyll equations for acetone, methanol and

708 ethanol solvents, *Photosynth. Res.*, 89, 27-41, 2006.

709 Rogelj, J., Shindell, D., Jiang, K., Fifita, S., Forster, P., Ginzburg, V., Handa, C., Kheshgi, H., Kobayashi,
710 S., Kriegler, E., Mundaca, and L., S., R., and Vilarino, M. V: Mitigation Pathways Compatible with
711 1.5°C in the Context of Sustainable Development, in: *Global Warming of 1.5°C: IPCC Special*
712 *Report on Impacts of Global Warming of 1.5°C above Pre-industrial Levels in Context of*
713 *Strengthening Response to Climate Change, Sustainable Development, and Efforts to Eradicate*
714 *Poverty*, edited by: Intergovernmental Panel on Climate, C., Cambridge University Press,
715 Cambridge, 93-174, DOI: 10.1017/9781009157940.004, 2022.

716 Rokitta, S. D., John, U., and Rost, B.: Ocean acidification affects redox-balance and ion-homeostasis in
717 the life-cycle stages of *Emiliana huxleyi*, *Plos One*, 7, e52212, 2012.

718 Schulz, K. G., Bellerby, R. G. J., Brussaard, C. P. D., Büdenbender, J., Czerny, J., Engel, A., Fischer, M.,
719 Koch-Klavsen, S., Krug, S. A., Lischka, S., Ludwig, A., Meyerhöfer, M., Nondal, G., Silyakova, A.,
720 Stuhr, A., and Riebesell, U.: Temporal biomass dynamics of an Arctic plankton bloom in response
721 to increasing levels of atmospheric carbon dioxide, *Biogeosciences*, 10, 161-180, 10.5194/bg-10-
722 161-2013, 2013.

723 Steidinger, K. A. and Jangen, K.: Chapter 3 - Dinoflagellates, in: *Identifying Marine Phytoplankton*,
724 edited by: Tomas, C. R., Academic Press, San Diego, 387-584, [https://doi.org/10.1016/B978-](https://doi.org/10.1016/B978-012693018-4/50005-7)
725 [012693018-4/50005-7](https://doi.org/10.1016/B978-012693018-4/50005-7), 1997.

726 Stukel, M. R., Irving, J. P., Kelly, T. B., Ohman, M. D., Fender, C. K., and Yingling, N.: Carbon
727 sequestration by multiple biological pump pathways in a coastal upwelling biome, *Nat. Commun.*,
728 14, 2024, 10.1038/s41467-023-37771-8, 2023.

729 Tanaka, T., Alliouane, S., Bellerby, R. G. B., Czerny, J., de Kluijver, A., Riebesell, U., Schulz, K. G.,
730 Silyakova, A., and Gattuso, J. P.: Effect of increased $p\text{CO}_2$ on the planktonic metabolic balance
731 during a mesocosm experiment in an Arctic fjord, *Biogeosciences*, 10, 315-325, 10.5194/bg-10-
732 315-2013, 2013.

733 Taylor, A. R., Brownlee, C., and Wheeler, G.: Coccolithophore cell biology: chalking up progress, *Annu.*
734 *Rev. Mar. Sci.*, 9, 283-310, 2017.

735 Thingstad, T. F. and Rassoulzadegan, F.: Nutrient limitations, microbial food webs and 'biological C-
736 pumps': suggested interactions in a P-limited Mediterranean, *Mar. Ecol. Prog. Ser.*, 117, 299-306,

737 1995.

738 Thingstad, T. F. and Rassoulzadegan, F.: Conceptual models for the biogeochemical role of the photic
739 zone microbial food web, with particular reference to the Mediterranean Sea, *Prog. Oceanogr.*, 44,
740 271-286, [https://doi.org/10.1016/S0079-6611\(99\)00029-4](https://doi.org/10.1016/S0079-6611(99)00029-4), 1999.

741 Vázquez, V., León, P., Gordillo, F. J. L., Jiménez, C., Concepción, I., Mackenzie, K., Bresnan, E., and
742 Segovia, M.: High-CO₂ Levels Rather than Acidification Restrict *Emiliana huxleyi* Growth and
743 Performance, *Microb. Ecol.*, 86, 127-143, [10.1007/s00248-022-02035-3](https://doi.org/10.1007/s00248-022-02035-3), 2023.

744 Wang, N. and Gao, K.: Ocean acidification and food availability impacts on the metabolism and grazing
745 in a cosmopolitan herbivorous protist *Oxyrrhis marina*, *Front. Mar. Sci.*, Volume 11 - 2024,
746 [10.3389/fmars.2024.1371296](https://doi.org/10.3389/fmars.2024.1371296), 2024.

747 Wu, Y., Campbell, D. A., and Gao, K.: Short-term elevated CO₂ exposure stimulated photochemical
748 performance of a coastal marine diatom, *Mar. Environ. Res.*, 125, 42-48,
749 <https://doi.org/10.1016/j.marenvres.2016.12.001>, 2017.

750 Yang, S. and Liu, X.: Characteristics of phytoplankton assemblages in the southern Yellow Sea, China,
751 *Mar. Pollut. Bull.*, 135, 562-568, 2018.

752 Yuan, Z., Liu, D., Masqué, P., Zhao, M., Song, X., and Keesing, J. K.: Phytoplankton Responses to
753 Climate-Induced Warming and Interdecadal Oscillation in North-Western Australia, *Paleoceanogr.*
754 *Paleocl.*, 35, e2019PA003712, <https://doi.org/10.1029/2019PA003712>, 2020.

755 Zhong, Y., Liu, X., Xiao, W., Laws, E. A., Chen, J., Wang, L., Liu, S., Zhang, F., and Huang, B.:
756 Phytoplankton community patterns in the Taiwan Strait match the characteristics of their realized
757 niches, *Prog. Oceanogr.*, 186, 102366, 2020.